Purdue University
Purdue e-Pubs

Purdue Energetics Research Center Articles | Purdue Energetics Research Center

2-2013

Thermal And Mechanical Response Of PBX 9501 Under Contact Excitation

J O. Mares
Purdue University

J K. Miller
Purdue University

N D. Sharp
Purdue University

D S. Moore
Moore Shock Spectra

D E. Adams
Purdue University

See next page for additional authors

Follow this and additional works at: https://docs.lib.purdue.edu/perc_articles

Recommended Citation
J. O. Mares, J. K. Miller, N. D. Sharp, D. S. Moore, D. E. Adams, L. J. Groven, J. F. Rhoads, S. F. Son, "Thermal and mechanical response of PBX 9501 under contact excitation," Journal of Applied Physics, Vol. 113(8), p. 08904 (2013). dx.doi.org/10.1063/1.4793495

This document has been made available through Purdue e-Pubs, a service of the Purdue University Libraries. Please contact epubs@purdue.edu for additional information.

Authors
J O. Mares, J K. Miller, N D. Sharp, D S. Moore, D E. Adams, L J. Groven, J F. Rhoads, and Steven F. Son

This article is available at Purdue e-Pubs: https://docs.lib.purdue.edu/perc_articles/12

Thermal and mechanical response of PBX 9501 under contact excitation

J. O. Mares, J. K. Miller, N. D. Sharp, D. S. Moore, D. E. Adams, L. J. Groven, J. F. Rhoads, and S. F. Son

Citation: Journal of Applied Physics **113**, 084904 (2013);
View online: https://doi.org/10.1063/1.4793495
View Table of Contents: http://aip.scitation.org/toc/jap/113/8
Published by the American Institute of Physics

Articles you may be interested in

Heat generation in an elastic binder system with embedded discrete energetic particles due to high-frequency, periodic mechanical excitation
Journal of Applied Physics **116**, 204902 (2014); 10.1063/1.4902848

The impact of crystal morphology on the thermal responses of ultrasonically-excited energetic materials
Journal of Applied Physics **119**, 024903 (2016); 10.1063/1.4939812

Energy localization in HMX-Estane polymer-bonded explosives during impact loading
Journal of Applied Physics **111**, 054902 (2012); 10.1063/1.3688350

Phenomenological model of shock initiation in heterogeneous explosives
The Physics of Fluids **23**, 2362 (2008); 10.1063/1.862940

Thermal and mechanical response of particulate composite plates under inertial excitation
Journal of Applied Physics **116**, 244904 (2014); 10.1063/1.4904439

Ignition criterion for heterogeneous energetic materials based on hotspot size-temperature threshold
Journal of Applied Physics **113**, 064906 (2013); 10.1063/1.4792001

Thermal and mechanical response of PBX 9501 under contact excitation

J. O. Mares,[1] J. K. Miller,[2] N. D. Sharp,[2] D. S. Moore,[3] D. E. Adams,[2] L. J. Groven,[2] J. F. Rhoads,[2] and S. F. Son[2]
[1]*School of Aeronautics and Astronautics, Purdue University, West Lafayette, Indiana 47907, USA*
[2]*School of Mechanical Engineering, Purdue University, West Lafayette, Indiana 47907, USA*
[3]*Moore Shock Spectra, Santa Fe, New Mexico 87508, USA*

(Received 11 December 2012; accepted 11 February 2013; published online 25 February 2013)

The thermal and mechanical responses of a cyclotetramethylene-tetranitramine-based explosive (PBX 9501) and two non-energetic mock materials (900-21 and PBS 9501) under high-frequency mechanical excitation are presented. Direct contact ultrasound transducers were used to excite samples through a frequency range of 50 kHz to 40 MHz. The mechanical response of each sample was approximated from a contact receiving transducer and trends were confirmed via laser Doppler vibrometry. The steady-state thermal response of the samples was measured at discrete excitation frequencies via infrared thermography. A maximum temperature rise of approximately 15 K was observed in PBX 9501, and the mock materials exhibited similar thermal characteristics. Temperature gradients were calculated to estimate the total heat generated within the samples due to the mechanical excitation. The active heating mechanisms were found to be highly dependent on the frequency of excitation. Possible mechanisms of heating at frequencies below 1 MHz are likely related to bulk motion. Above this frequency, the active heating mechanisms are likely related to particle-scale processes. The observed phenomena may prove useful in the aid of current trace vapor detection methods for explosives. © *2013 American Institute of Physics*.
[http://dx.doi.org/10.1063/1.4793495]

I. INTRODUCTION

The stand-off detection of composite explosives or homemade explosive compositions by trace vapor detection methods remains a tremendous challenge.[1] This is largely due to the combination of low material vapor pressures and a highly dynamic detection environment, which results in very low vapor concentrations. It is well documented that the vapor pressures of many explosive materials are highly dependent on temperature and may be substantially raised by minor temperature increases.[2] Thus, using mechanical excitation as a means to induce heat and increase vapor pressures is of particular interest. This could enable potential pathways for both stand-off detection (through the examination of outgassing of vapors) and for stand-off defeat (through the remote triggering of deflagration).[3] Conceptually, this could be achieved through the heating of the targeted explosives via an external source, such as ultrasound radiation. Despite this potential, the thermal response of composite explosives to high-frequency mechanical stimulation has yet to be thoroughly studied.

In prior work, Loginov[4,5] observed that applying low-frequency mechanical vibrations to certain neat energetic materials produced thermal responses that were strongly dependent on the frequency of excitation. Explosives such as cyclotrimethylenetrinitramine (RDX) and lead azide were driven to initiation under certain excitation conditions. Other studies found that the reaction of energetic materials may be stimulated by ultrasonic radiation;[6–8] but only if the explosives were submerged in a liquid, as microscale cavitation effects were believed to be the primary cause of initiation. Sutherland and Kennedy[9] conducted high-frequency acoustic wave experiments on cyclotetramethylene-tetranitramine (HMX) and triaminotrinitrobenzene (TATB) based explosives and observed evidence of binder decomposition during excitation. Although the decomposition was attributed to the slight thermal cycling of the material, heating effects due to the high-frequency acoustic insult appear to be a more plausible explanation.

In commercial and medical applications, heating induced by high-frequency mechanical excitation is a specifically utilized effect and recent efforts have been made to characterize the causes of this heating. For example, the mechanisms of heat generation in vibrothermography[10,11] have been explored by Renshaw *et al.*[12] in titanium, aluminum, and carbon reinforced composite samples. They showed experimental evidence of heating due to friction at crack interfaces, plastic deformation, and viscoelastic dissipation due to bulk cyclic motion. In the field of ultrasonic welding, which utilizes high-power mechanical excitation to fuse plastics, Tolunay *et al.*[13] claimed that friction and viscous dissipation due to bulk motion are the major mechanisms that contribute to heating. In explosive materials, these fundamental mechanisms have not been explored.

The objectives of this work were to observe and characterize the thermal and mechanical responses of PBX 9501 (a plastic-bonded HMX-based explosive) and two mechanical mock materials (PBS 9501 and 900-21) under mechanical excitations in the range of 50 kHz to 40 MHz. Direct contact excitation was used in order to transfer the highest possible energies into the targeted materials. Heat generation induced via external excitation was quantified at discrete excitation frequencies. The dependence of heat generation on excitation frequency was investigated and two principle heating mechanisms were proposed.

 © 2013 American Institute of Physics

TABLE I. Material composition and properties.

Material	Composition (wt. %) HMX	$Ba(NO_3)_2$	Pentek	Sugar (C&H)	Estane	BDNPA-F	Relevant material properties: Theoretical maximum density (g/cm^3)	Thermal conductivity (W/m K)
PBX 9501 (Ref. 16)	95.00	…	…	…	2.5	2.5	1.86	0.454
900-21 (Ref. 17)	…	44.65	49.35	…	3.0	3.0	1.861	0.679
PBS 9501 (Ref. 18)	…	…	…	94.00	3.0	3.0	1.57	1.18

II. EXPERIMENTAL TECHNIQUE

A. Materials and sample preparation

Three materials were studied: PBX 9501 and two representative non-energetic mechanical mocks, 900-21 and PBS 9501. PBX 9501 and 900-21 molding powders were obtained from Los Alamos National Laboratory (LANL) and PBS 9501 molding powder was prepared following the procedures outlined in Liu.[14] The compositions of these materials are listed in Table I. The mock material 900-21 uses the same binder composition and matches the density of PBX 9501, whereas the mock material PBS 9501 uses the same binder composition and closely matches the initial particle sizes of PBX 9501. The thermal properties of the mock materials were measured utilizing the transient plane source technique.[15] A uniaxial die set and high-pressure press were used to form cylindrical pellets of each composite material with nominal diameters and lengths of 1.27 cm. The average theoretical mass density of the PBX 9501, 900-21, and PBS 9501 samples used in this study were 97%, 98%, and 97%, respectively.

B. Mechanical excitation and measurement

Contact ultrasound transducers, as listed in Table II, were affixed to each cylindrical sample with Devcon® 5 Minute Epoxy and were cured for at least 24 h. Each transducer is listed as ideally exciting in the "axial" or "radial" mode; however, each transducer generated a variety of wave types. One "driving" transducer was supplied with a sinusoidal signal at a nominal voltage of 20 Vpp by a Fluke 294 Series Waveform Generator. The supplied excitation signal and the signal generated by the "receiving" transducer were measured with a Tektronix DPO 4034 oscilloscope. The excitation signal frequency was swept in both rising and falling directions from 50 kHz to 40 MHz with an overall sweep time on the order of 30 min. The sample was suspended by the electrical leads during testing in order to limit thermal and mechanical boundary effects.

In addition, laser Doppler vibrometry (LDV) was used to recover optical measurements of the velocities and deflections of the mechanically excited samples. Test specimens for these measurements were prepared with only one affixed driving transducer, leaving one end bare. The sample was supported by highly compliant foam to mimic free boundary conditions and to attenuate interference due to background vibrations. The driving ultrasound transducer was excited by broadband noise up to 1 MHz at an excitation level of 40 Vpp while the mechanical response of the samples was measured using a Polytec PSV-400 scanning vibrometer. Note that the excitation level employed for the LDV measurements was distinct from the transducer response measurements. The excitation signal was supplied by the waveform generator used in concert with a Kron-Hite 7500 power amplifier. Spatial averaging of optical measurements was performed over 750 points on the free face and 55 points along the longitudinal axis, yielding frequency-domain measurements of the sample's bulk mechanical response.

C. Thermal measurements

A forward-looking infrared FLIR A320 thermal camera with a temperature sensitivity of 0.07 K at 303 K and accuracy of ±2 K or ±2% of the reading was used to measure the thermal response of the mechanically excited sample at discrete excitation frequencies, as shown in Figure 1. The temperature measurements for each sample material were calibrated through the use of a hot plate and a reference thermocouple. Excitation frequencies were selected through an initial log-spaced sweep, with additional frequencies evaluated to resolve peaks in the thermal response. The driving excitation signal was again nominally 20 Vpp. Thermal equilibrium was defined as the state in which the average sample temperature changed less than one-half Kelvin over 100 s. The spatial resolution of the IR camera was approximately 0.25 mm per pixel. A representative thermal image of a mechanically excited sample is shown in Figure 2. Ambient temperature fluctuations were measured during testing and used to correct the sample temperature measurements.

To validate the thermal analysis technique used in this study, conductive heating studies were also performed. The experimental set-up was similar to the thermal studies described

TABLE II. Transducer properties.

Name	Manufacturer	Transducer	Resonance frequency (kHz)	Active mode	Material
215R	Steiner & Martins, Inc.	SMD10T2R111	215 ± 3%	Radial	Modif. PZT-4
3400A	Steiner & Martins, Inc.	SMD12T06R412WL	3400 ± 5%	Axial	PZT-5A

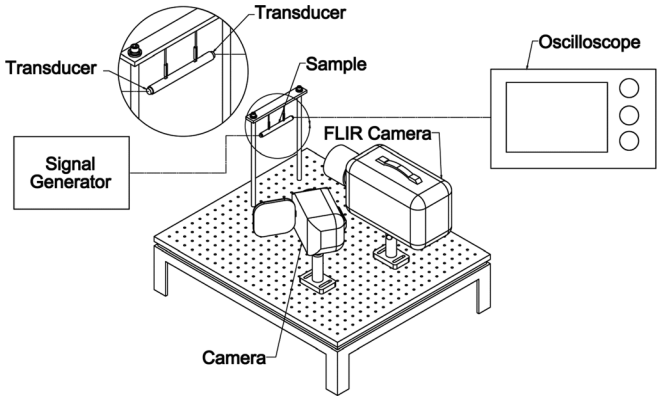

FIG. 1. Experimental schematic for thermal and mechanical response experiments. The Fluke 294 waveform generator excites each sample-transducer system, while a FLIR A320 thermal camera and Tektronix DPO 4034 Oscilloscope record the thermal and electrical responses, respectively.

previously except that there was no mechanical excitation. A rubber-coated heating element was attached to the sample end to raise the temperature of the samples to the levels observed during mechanical excitation. These tests were used as a control case in which no heat generation occurred within the sample.

III. RESULTS AND DISCUSSION

A. Mechanical response

The mechanical response of each sample was investigated to determine the dependence of heat generation on the bulk motion of the sample. To characterize the level of deflection experienced by the sample during excitation, the signal generated by the "receiving" transducer was used to characterize the level of bulk motion of the sample. The amplitudes of these response signals are presented as a function of the excitation frequency in Figures 3–5. Due to the differing mass, geometry, and material of the contact transducers, the resulting observed mechanical response is unique for each transducer/sample system.

For both the 215R and 3400A transducers, the general trends of the PBX 9501 samples exhibit major structural resonances of the transducer/sample system near 220 kHz, while the response amplitudes at frequencies above 1 MHz are relatively small (see Figure 3). This result illustrates that bulk motion of the sample occurs at frequencies lower than 1 MHz, and that little wave propagation through the sample is recorded above this frequency. The general trend of the mechanical response of the PBX 9501 samples is similar to the trends exhibited by the mock samples, 900-21 and PBS 9501 (see Figures 4 and 5). While each sample was of similar

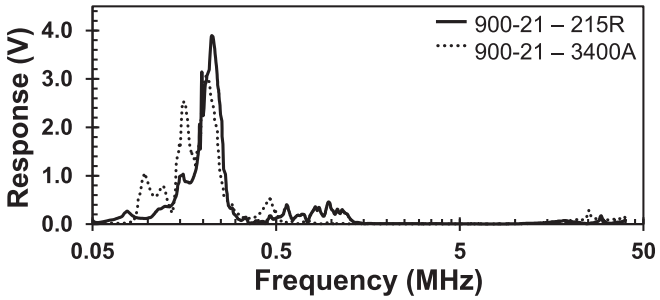

FIG. 3. Frequency response of PBX 9501 excited and measured by the listed transducers. The level of electrical excitation was nominally 20 Vpp.

geometry and binder composition, differences in the chemical composition and sizes of the particles contribute to observable differences in the detailed mechanical responses. It is important to note that multiple trials with replicate transducers and samples were performed and frequency-specific results were found to be repeatable. It should also be noted that for all cases, the system experienced an electromechanical resonance within the examined frequency range that affected the voltage supplied to the driving transducer. The frequency of this resonance does not correspond to any of the thermal or mechanical results of interest presented in this paper.

Laser Doppler vibrometry was used to evaluate the merit of characterizing the bulk motion of the sample via the transducer response. As shown in Figure 6, the LDV measurements captured trends similar to the transducer response, even with the slight differences in the excitation and boundary conditions that were present. This result suggests that the measured transducer response effectively captures the bulk motion of the sample. Bandwidth limitations of the LDV system prevent measurements above 1 MHz, and thus the transducer responses alone were used to represent the bulk motion of the samples over the full range of frequencies tested. As expected, wave propagation through the sample was observed via the LDV at the dominant structural resonance as illustrated by the representative experimental deflection shape shown in Figure 7. Heating within the material was expected at this resonance due to the high level of bulk motion experienced by the sample.

B. Thermal response

To evaluate the level of heat generation within the sample, the steady-state surface temperatures of the mechanically excited samples were recorded. These temperatures were averaged radially, generating profiles as functions of longitudinal position. The temperature profiles are shown for all transducer/sample systems at each investigated frequency

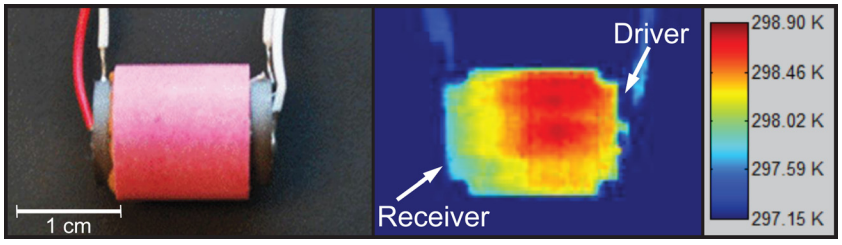

FIG. 2. Representative image of a 900-21 sample compared to an IR image of the excited sample with the indicated temperature excursion.

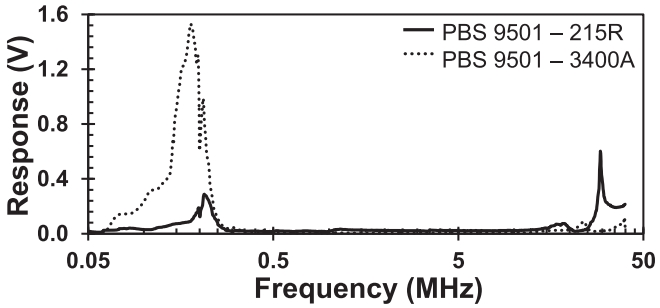

FIG. 4. Frequency response of 900-21 mock excited and measured by the listed transducers. The level of electrical excitation was nominally 20 Vpp.

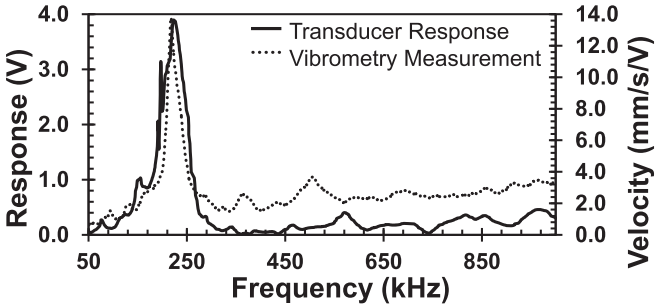

FIG. 6. Frequency response of 900-21 mock excited and measured by 215R transducers compared to the LDV velocity measurement.

in Figure 8. Interestingly, the temperature profiles at the dominant structural resonance frequency indicate that the maximum thermal rise occurs within the sample at some distance from the driving transducer, suggesting that heat is generated within the sample.

All samples excited by the 3400A transducer exhibit a secondary maximum thermal rise near 4 MHz. Samples excited by the 215R transducer also exhibit thermal maxima at frequencies above the dominant structural resonance; however, these responses are not centered about one frequency. At these higher-frequencies, the location of the maximum temperature within the sample is near the active transducer. This suggests that the higher frequency waves become quickly dispersed by the material and fail to fully propagate throughout the sample, as evident by the mechanical response results. For all materials, the excitation induced by the 215R transducer achieves a maximum thermal rise of approximately 3 K. A maximum thermal rise of approximately 15 K was observed in PBX 9501 while excited by the 3400A transducer, and this temperature rise was observed in the PBS 9501 mock sample.

The thermal responses of the samples can be attributed to the mechanical excitation as well as Ohmic heating of the transducer. As Ohmic heating of the transducer only influenced the sample via conduction, heat generated within the sample is solely attributed to the mechanical excitation. Thus, the effects of Ohmic heating are intrinsically excluded in heat generation analysis.

To quantify heat generation, the 2D temperature measurements were assumed to represent the temperature distributions of the axial plane through the cylindrical sample. Temperature gradients at the sample boundary in the direction normal to the surface were evaluated using a forward divided difference formula

$$\begin{aligned}\frac{dT}{dx} &= \frac{[-3T(x_{i+2}) + 4T(x_{i+1}) - T(x_i)]}{2\Delta x}, \quad \text{(Face surface)},\\ \frac{dT}{dr} &= \frac{[-3T(r_{i+2}) + 4T(r_{i+1}) - T(r_i)]}{2\Delta r}, \quad \text{(Radial surface)},\end{aligned} \tag{1}$$

where x_i and r_i are locations at the boundary, x_{i+1} and r_{i+1}, x_{i+2} and r_{i+2} are sequential locations within the sample normal to the boundary, and Δx and Δr are the distances between each location in the axial or radial direction of the boundary normal.

Noting that the thermal data were recorded while the sample is at steady-state, the heat flux can be calculated via Fourier's law of conduction

$$\dot{q} = -k\nabla T, \tag{2}$$

where $\dot{q}$ is the heat flux, k is the sample's thermal conductivity, and T is temperature. This can be represented in a one-dimensional form as

$$\begin{aligned}\dot{Q}_{out} &= -kA_{appl}\frac{dT}{dx}, \quad \text{(Face surface)},\\ \dot{Q}_{out} &= -kA_{appl}\frac{dT}{dr}, \quad \text{(Radial surface)},\end{aligned} \tag{3}$$

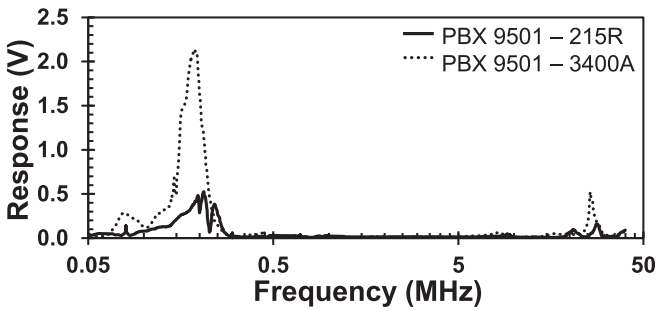

FIG. 5. Frequency response of PBS 9501 excited and measured by the listed transducers. The level of electrical excitation was nominally 20 Vpp.

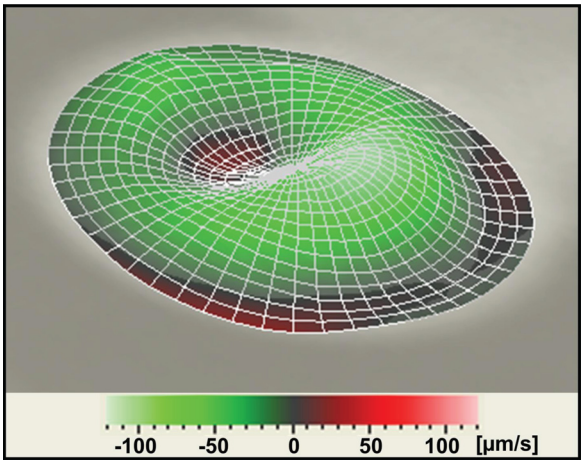

FIG. 7. Vibrometry-recorded experimental deflection shape of a 900-21 cylinder at 220 kHz with 215R transducer.

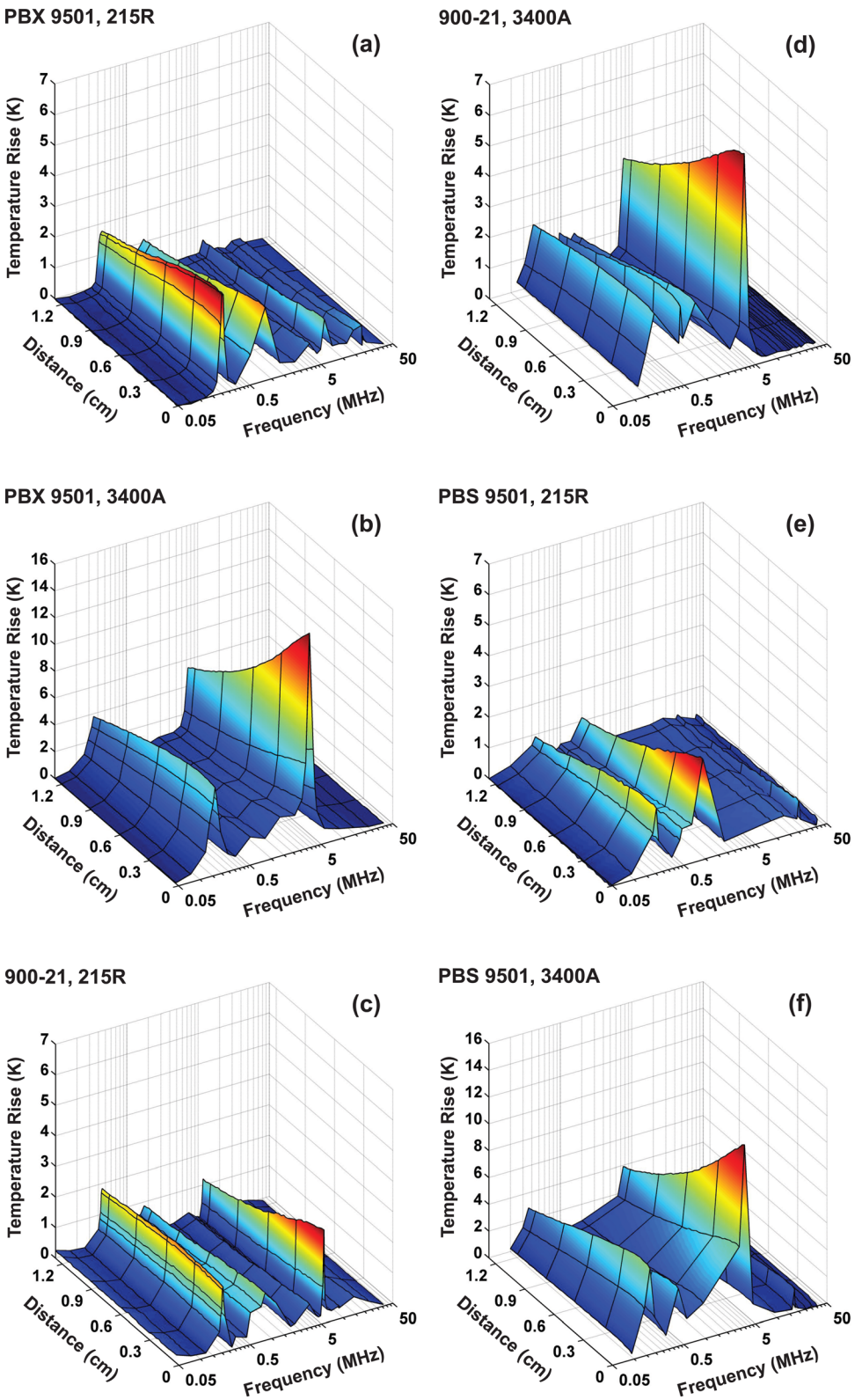

FIG. 8. Temperature excursion vs. frequency and distance from transducer edge. Data color is weighted by temperature excursion. The spatial resolution is 0.24 mm, the temperature resolution is 0.1 K, and frequency data are a collection of discrete sets indicated by transverse lines with shaded linear connecting surfaces. Data are presented for the following transducer/sample systems: (a) PBX 9501, 215R; (b) PBX 9501, 3400A; (c) 900-21, 215R; (d) 900-21, 3400A; (e) PBS 9501, 215R; and (f) PBS 9501, 3400A. Note the differences in temperature scale between the various cases.

where $\dot{Q}_{out}$ is the heat transfer rate in the outward boundary normal direction, A_{appl} is the applicable boundary surface area, and dT/dx and dT/dr are the temperature gradients in the appropriate boundary normal directions. Note that the applicable area was defined as the surface area of the cylinder that the boundary represents and was evaluated by revolving the distance Δx or Δr about the cylinder axis.

The steady-state heat transfer rate at the surface of the sample was then evaluated using Eq. (3). The total summed heat transfer rate through each boundary was then defined as the amount of heat generated within the sample as follows:

$$\dot{Q}_{gen} = \sum \dot{Q}_{out}, \tag{4}$$

where $\dot{Q}_{gen}$ is the estimated amount of heat generated.

In order to validate this method, the thermal data from the conductive heating control experiments were evaluated.

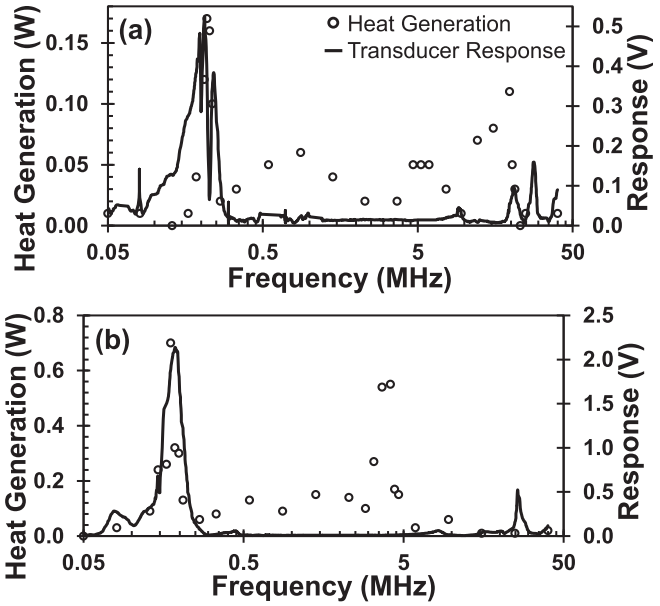

FIG. 9. Heat generation within sample vs. frequency for PBX 9501 with transducers: (a) 215R and (b) 3400A.

Each case yielded no level of heat generation outside of the experimental error.

The levels of heat generation produced by the mechanical excitation at discrete frequencies are shown with the mechanical response in Figures 9–11. In each case, below 1 MHz, the level of heat generation is strongly correlated to the level of bulk mechanical response. The heating observed in this lower frequency regime is, thus, attributed to the bulk motion of the material. This is likely a result of viscoelastic losses, as well as thermoelastic dissipation. Above this frequency threshold, significant levels of heat generation occur with little correlation to the bulk mechanical response. These occurrences of significant heat generation are localized in

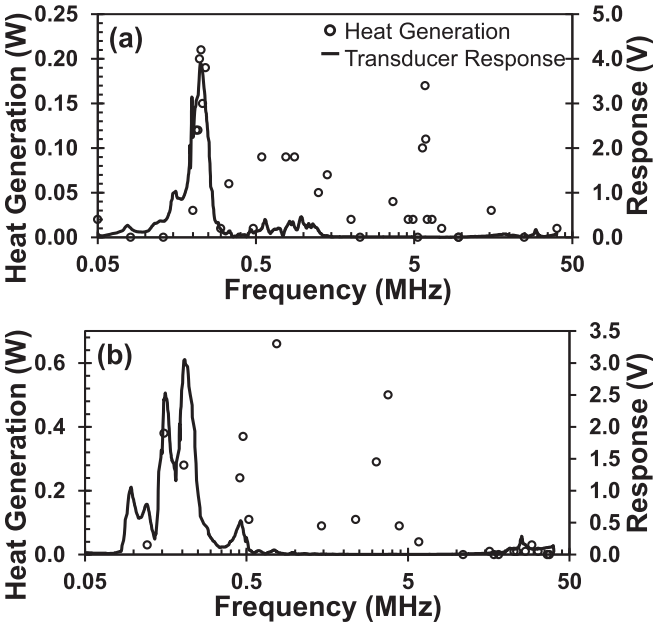

FIG. 10. Heat generation within sample vs. frequency for 900-21 with transducers: (a) 215R and (b) 3400A.

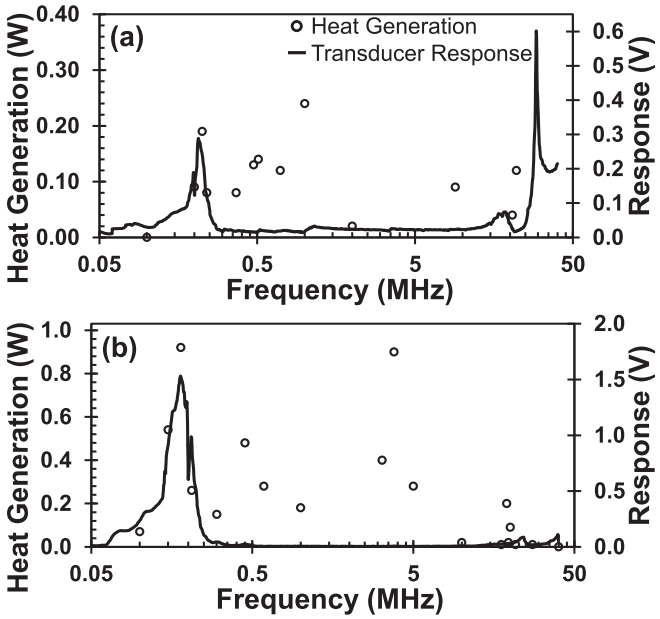

FIG. 11. Heat generation within sample vs. frequency for PBS 9501 with transducers: (a) 215R and (b) 3400A.

narrow frequency bands and may be linked to interactions on the particle scale.

Skidmore *et al.*[19] report that the post-pressing mean particle size of PBX 9501 is approximately 200 μm. Likewise, Dick *et al.*[20] report the bulk wave speed for PBX 9501 as 2500 m/s. Accordingly, the excitation wavelength approaches the particle size of HMX for frequencies on the order of 10 MHz. As the wavelength approaches the size of the particles within the material, it is postulated that the deflection between neighboring particles is maximized. Thus, particle scale processes such as increased viscoelastic losses of the binder between particles, frictional effects due to particle-particle interactions, and localized thermoelastic effects may contribute to heating at higher frequencies. As multiple wave types exist in solid composite materials, multiple frequencies may be targeted to induce significant heating effects by these particle scale interactions. In all PBX 9501 trials, multiple high-frequency thermal peaks appear in support of this length scale approximation. As the materials 900-21 and PBS 9501 are mechanical mocks for PBX 9501, the particle sizes are on the same order as the HMX particles used in PBX 9501. The bulk wave speeds of 900-21 and PBS 9501 were estimated to be on the order of 2400 m/s and 1500 m/s, respectively, through simple time of flight measurements. The excitation wavelengths for these materials are estimated to approach the particle sizes near similar frequencies to PBX 9501. Thus, the significant heat generation results at frequencies above the 1 MHz threshold observed for both 900-21 and PBS 9501 imply the same phenomena.

IV. CONCLUSIONS

The mechanical and thermal responses of PBX 9501 and two respective mock materials (PBS 9501 and 900-21) under direct ultrasonic excitation are presented for the first time. The mechanical response of each sample was similar,

suggesting a dominant mechanical resonance of the transducer/sample system near 200 kHz.

The active mechanism(s) causing heat generation under mechanical excitation for these highly heterogeneous materials have yet to be fully characterized; however, experimental observations clearly indicate that the mechanism(s) are dependent on the excitation frequency. Below a frequency limit of 1 MHz, the major mechanisms of heat generation are proposed to be viscoelastic losses and thermoelastic dissipation. The mechanisms of heat generation at frequencies beyond this limit must occur on the particle scale, and multiple mechanisms are suggested. The estimated wavelength of this high-frequency excitation would induce heating on the particle scale, but optical limits of the thermal camera system allow observation only at the bulk scale.

Exploitation of these heating mechanisms under high-frequency mechanical excitations has proven effective in heating a composite energetic material, PBX 9501. Through the utilization of ultrasound radiation at specific target frequencies of excitation, significant thermal responses may potentially be induced in energetic materials from a stand-off source. This could allow for greater success in current vapor trace explosives detection methods and lead to a unique stand-off method of defeat for explosives.

Further work should attempt to elucidate the specific heating mechanisms that exist at various frequencies. Microscale vibrometry and thermography should be employed to attempt characterization of the relations between the mechanical and thermal responses at the particle scale.

ACKNOWLEDGMENTS

This research was supported by the U.S. Office of Naval Research under the Multidisciplinary University Research Initiative on "Sound and electromagnetic interacting waves" (through Grant No. N00014-10-1-0958) and under the Basic Research Challenge on "Chemical decomposition in high energy density materials induced by coupled acoustic electromagnetic energy insult" (through Grant No. N00014-11-1-0466). J.O.M. also wishes to acknowledge the National Science Graduate Research Fellowship Program and the Purdue Doctoral Fellowship program.

[1]D. S. Moore, Rev. Sci. Instrum. **75**, 2499 (2004).
[2]D. S. Moore, Sens. Imaging **8**, 9 (2007).
[3]D. S. Moore, "Method and apparatus for detecting explosives," U.S. patent 7,939,803 (2011).
[4]N. P. Loginov, S. M. Muratov, and N. K. Nazarov, Combust., Explos. Shock Waves **12**, 367 (1976).
[5]N. P. Loginov, Combust., Explos. Shock Waves **33**, 598 (1997).
[6]V. Bobolev and J. Chariton, Acta Physicochim. URSS **7**, 416 (1937).
[7]V. Griffing and A. Macek, Trans. Faraday Soc. **50**, 1331 (1954).
[8]F. A. H. Rice and D. Levine, Proc. R. Soc. London A **246**, 180 (1958).
[9]H. J. Sutherland and J. E. Kennedy, J. Appl. Phys. **46**, 2439 (1975).
[10]V. P. Vavilov and D. A. Nesteruk, Russ. J. Nondestr. Test. **46**, 147 (2010).
[11]R. B. Mignogna, R. E. Green, Jr., J. C. Duke, Jr., E. G. Henneke II, and K. L. Reifsnider, Ultrasonics **19**, 159 (1981).
[12]J. Renshaw, J. C. Chen, S. D. Holland, and R. B. Thompson, NDT & E Int. **44**, 736 (2011).
[13]M. N. Tolunay, P. R. Dawson, and K. K. Wang, Polym. Eng. Sci. **23**, 726 (1983).
[14]C. Liu, in SEM Annual Conference and Exposition on Experimental and Applied Mechanics, Jun 4–7 2006, Saint Louis, MO, United States (2006).
[15]S. E. Gustafsson, Rev. Sci. Instrum. **62**, 797 (1991).
[16]T. R. Gibbs and A. Popolato, *LASL Explosive Property Data* (University of California Press, Berkeley, CA, 1980).
[17]C. Liu, C. M. Cady, P. J. Rae, and M. L. Lovato, in Proceedings of the 14th International Detonation Symposium, Apr 11–16 2012, Coeur d'Alene, ID, United States (2010).
[18]P. J. Rae, D. M. Williamson, and J. Addiss, Exp. Mech. **51**, 467 (2011).
[19]C. B. Skidmore, D. S. Phillips, S. F. Son, and B. W. Asay, AIP Conf. Proc. **429**, 579–582 (1998).
[20]J. J. Dick, A. R. Martinez, and R. S. Hixson, "Plane impact response of PBX 9501 and its components below 2 GPa," Technical Report No. LA-13426-MS (Los Alamos National Laboratory, 1998).